ELSEVIER

Contents lists available at ScienceDirect

## Earth and Planetary Science Letters

www.elsevier.com/locate/epsl



# Stability of calcium and magnesium carbonates at Earth's lower mantle thermodynamic conditions



Samuel S.M. Santos <sup>a,\*</sup>, Michel L. Marcondes <sup>a,1</sup>, João F. Justo <sup>b</sup>, Lucy V.C. Assali <sup>a</sup>

- <sup>a</sup> Instituto de Física, Universidade de São Paulo, CEP 05508-090, São Paulo, SP, Brazil
- <sup>b</sup> Escola Poliécnica, Universidade de São Paulo, CEP 05424-970, São Paulo, SP, Brazil

#### ARTICLE INFO

Article history:
Received 12 April 2018
Received in revised form 12 October 2018
Accepted 16 October 2018
Available online 29 October 2018
Editor: M. Bickle

Keywords: carbonates high-pressure minerals high-temperature minerals lower mantle

#### ABSTRACT

We present a theoretical investigation, based on ab initio calculations and the quasi-harmonic approximation, on the stability properties of magnesium (MgCO<sub>3</sub>) and calcium (CaCO<sub>3</sub>) carbonates at high temperatures and pressures. The results indicate that those carbonates should be stable in the Earth's lower mantle, instead of dissociating into other minerals, in chemical environments with excess of SiO<sub>2</sub>, MgO, or MgSiO<sub>3</sub>. Therefore, considering the lower mantle chemical composition, consisting mostly of the MgSiO<sub>3</sub> and MgO minerals, calcium and magnesium carbonates are the primary candidates as carbon hosts in that region. For the thermodynamic conditions of the mantle, the results also indicate that carbon should be primarily hosted on MgCO<sub>3</sub>, contrasting with what was found by other theoretical studies, which neglected temperature effects. Finally, the results indicate that carbon, in the form of free CO<sub>2</sub>, is unlikely in the lower mantle.

© 2018 Elsevier B.V. All rights reserved.

#### 1. Introduction

Carbon is a unique chemical element, mainly due to its rich bonding nature, which provides a wide range of stable and metastable structures in several hybridizations and configurations. Particularly, the role of carbon on Earth's natural phenomena has been extensively studied over the last few decades. The carbon cycle affects the atmosphere, oceans, and other shallow crustal phenomena, directly influencing climate, ecosystems, and, consequently, life on Earth. Although there is considerable accumulated knowledge on the carbon cycle near the Earth's surface, there is still scarce information on the processes associated with its deep layers (Hazen and Schiffries, 2013).

In order to build consistent models on the Earth's carbon cycle, it is important to establish a proper understanding of its chemical composition. The knowledge on the solar system composition, based on information from carbonaceous chondritic meteorites that have hit the Earth, allows estimating the expected amount of carbon that should be present on Earth (Marty et al., 2013). However, the quantity of carbon currently known on its shallow layers is about two orders of magnitude smaller than the expected value, suggesting that this missing carbon should be stored on its deep

layers, the so-called deep carbon reservoirs (Hazen and Schiffries, 2013). Estimates indicate that the Earth's deep interior may contain as much as 90% of all available carbon. Such conclusions have been supported by indirect evidence, such as the presence of  $CO_2$  in magmas (Marty et al., 2013) and the mineral inclusions within natural deep diamonds (Walter et al., 2011; Pearson et al., 2014; Maeda et al., 2017).

There are several questions on the properties of deep carbon that remain open, such as determining the amount and distribution of those carbon reservoirs within major mantle minerals and understanding the complete carbon cycle, associated with an exchange of carbon between the Earth's surface and its deep interior. For example, current estimates suggest that the carbon flux into the Earth's mantle through subduction substantially exceeds the carbon flux emitted by volcanoes, opening the question on the minerals that host carbon in the mantle.

Those issues could only be addressed with a deep understanding of the behavior of carbon-related minerals under high pressures and temperatures, at the thermodynamic conditions of the mantle (Oganov et al., 2013). Although some carbon may be stored in the core, the mantle is thought to be its largest reservoir. It is reasonable to assume that a certain amount of carbon could be dissolved in silicates, such as MgSiO<sub>3</sub>, which is by far the most abundant mineral in the lower mantle. Therefore, even if carbon had a low to moderate solubility in this mineral, it could still be the largest carbon reservoir in that region. However, it has been experimentally shown that the carbon solubility in silicates is below

<sup>\*</sup> Corresponding author. E-mail address: sssamuel@usp.br (S.S.M. Santos).

<sup>&</sup>lt;sup>1</sup> Present address: Department of Earth and Environmental Sciences, Columbia University, Lamont-Doherty Earth Observatory, Palisades, NY 10964, USA.

30–200 ppb by weight (Shcheka et al., 2006), indicating that most of the Earth's carbon must be stored in other minerals. Furthermore, silicates are large diffuse reservoirs, which contrasts with the concentrated phases of the deep carbon identified as magma carbonates (Jones et al., 2013) and diamonds (Shirey et al., 2013), as well as carbon species emitted by volcanoes (Burton et al., 2013).

In the lower mantle, most of the carbon is in a reduced state, such as in form of diamond. However, the oxidized state, such as in carbonates, is possible in subducted slabs. To further explore the potential carriers of carbon, it is important to explore the physical properties of those minerals at lower mantle thermodynamic conditions, specially in terms of carbon-related stable phases. Several theoretical (Marcondes et al., 2016; Oganov et al., 2008; Pickard and Needs, 2015) and experimental (Fiquet et al., 2002; Isshiki et al., 2004) investigations have explored the high-pressure stability of major carbonates, such as MgCO<sub>3</sub>, CaCO<sub>3</sub>, and MgCa(CO<sub>3</sub>)<sub>2</sub>. However, there is still scarce information on those properties at high temperatures (Gavryushkin et al., 2017; Smith et al., 2018). Particularly for the lower mantle, such conditions would mean pressures up to 136 GPa and temperatures up to 3000 K.

This investigation explores the stability of carbonates, specially MgCO<sub>3</sub> and CaCO<sub>3</sub>, at lower mantle conditions. Here, we do not explore the MgCa(CO<sub>3</sub>)<sub>2</sub> mineral, since it is well established that it dissociates into MgCO3 and CaCO3 for pressures greater than a few GPa (Shirasaka et al., 2002). The results are obtained by first-principles total energy calculations, combined with the quasiharmonic approximation, in order to obtain the respective Gibbs free energies of the minerals in different crystalline phases, at high temperatures and pressures. We explore the stability of those carbonates, taking into account a number of crystalline phases that have been identified by recent theoretical and experimental investigations. Our results indicate that at high temperatures and high pressures MgCO<sub>3</sub> and CaCO<sub>3</sub> should be stable against dissociation into other minerals at several mantle conditions. Considering the chemical composition of the lower mantle, with major concentrations of MgSiO<sub>3</sub> and MgO, calcium and magnesium carbonates should be the primary candidates as carbon hosts in the lower mantle. However, at the thermodynamic conditions of the mantle, along its geotherm, magnesium carbonate is by far much more likely than calcium carbonate to host carbon. Additionally, the results suggest that carbon in the form of isolated CO2 is unlikely in the lower mantle.

## 2. Methods

#### 2.1. Ab initio calculations

The first principles calculations are performed using the Quantum ESPRESSO computational package (Giannozzi et al., 2009). The electronic interactions are described within the density functional theory, considering the exchange-correlation (XC) functional based on the local density approximation (LDA) (Kohn and Sham, 1965). This functional has been widely used to obtain both static and dynamic properties of the Earth's mantle minerals, although many authors have investigated those properties with the generalized gradient approximation (GGA-PBE) (Perdew et al., 1996). It is well established in the literature that static calculations with the LDA underestimate the mineral lattice parameters (generally by about 1 to 2%) and the phase transition pressures, and overestimate the respective elastic constants when compared to experimental values at finite temperatures, while calculations with the GGA-PBE provide the opposite effects (Marcondes et al., 2018). This investigation uses only the LDA functional as justified in detail in the next section.

The electronic wave functions are expanded using the projected augmented wave (PAW) method (Blochl, 1994), with a plane-wave

cutoff of 1200 eV. The valence electronic configurations are described with  $3s^23p^64s^23d^04p^0$  for calcium,  $2s^22p^2$  for carbon,  $2s^22p^63s^23p^0$  for magnesium,  $3s^23p^2$  for silicon, and  $2s^22p^4$  for oxygen (Holzwarth et al., 2001).

The Brillouin zones for computing the electronic properties are sampled by a  $4\times4\times4$  k-mesh for the carbonates and silicates, a  $8\times8\times8$  k-mesh for the alkaline earth oxides (MgO and CaO), and a  $6\times6\times6$  k-mesh for SiO<sub>2</sub> and CO<sub>2</sub>, in order to provide an approximately equivalent density of k-points for all materials.

Strict convergence criteria are taken into account for the simulations, with the atomic positions being considered converged when all forces acting on atoms are smaller than 0.01 eV  $\rm \mathring{A}^{-1}$ . For each pressure, from 0 to 150 GPa, the structures are optimized by using the damped variable cell shape molecular dynamics method (Wentzcovitch et al., 1993). Then, a third-order Birch–Murnaghan equation of state is used to fit the compression data.

#### 2.2. Thermodynamic properties

The thermodynamic properties are investigated by computing the vibrational modes (phonons) of the crystals using the Density Functional Perturbation Theory (Baroni et al., 2001), with a  $12 \times 12 \times 12$  q-mesh to calculate the vibrational density of states (VDOS) (Wang et al., 2010), and the quasi-harmonic approximation (QHA) (Wentzcovitch et al., 2010) to compute the respective Gibbs free energies.

The results for finite temperatures are reported within the validity range of the QHA (Wentzcovitch et al., 2010). It is well established in the literature that the QHA results for the thermal expansion,  $\alpha(P,T)$ , start diverging beyond a certain temperature, in contrast to available experimental results. Such divergence, in this methodology, is caused by disregarding anharmonic effects (Wentzcovitch et al., 2010, 2004). Moreover, this quantity is also clearly quite sensitive to the choice of the XC functional (Marcondes et al., 2018), and could still be used at high temperatures, providing results consistent with experimental data in the region in which the thermal expansion coefficient does not diverge. Therefore, at high temperatures, the validity region of the QHA has been established (Wentzcovitch et al., 2010; Carrier et al., 2007) as  $[\partial^2\alpha(P,T)/\partial T^2]_P \leq 0$ .

Fig. 1 shows the thermal expansion coefficient at several pressures for CaCO<sub>3</sub> in aragonite and post-aragonite phases, which represents a stringent test for this methodology, showing the respective validity regions of the QHA for those phases, indicating that, at very high pressures, the QHA is still valid at temperatures up to 3000 K. It can be observed that, within the validity limit of the QHA, the thermal expansion coefficient is in good agreement with available experimental data (Litasov et al., 2017). Additionally, Fig. 1(a) displays the thermal expansivity for aragonite obtained with the GGA-PBE functional, showing that the LDA results describe it well up to 800 K for null pressure, while the GGA-PBE results diverge much faster, decreasing the validity range of the QHA. These results provide an additional justification for using the LDA functional in this investigation.

We explore the validity of the QHA at the lowest pressure phases for all minerals considered in this investigation. The region of low pressures and high temperatures represents a stringent test for the QHA methodology since it is when the thermal expansion coefficients present major divergences when compared to experimental data. The QHA provides appropriate thermal expansion coefficients at the thermodynamic conditions of interest in this investigation.

Our results on thermal properties of all minerals investigated here are within the validity region of the QHA and in good agreement with available theoretical and experimental data

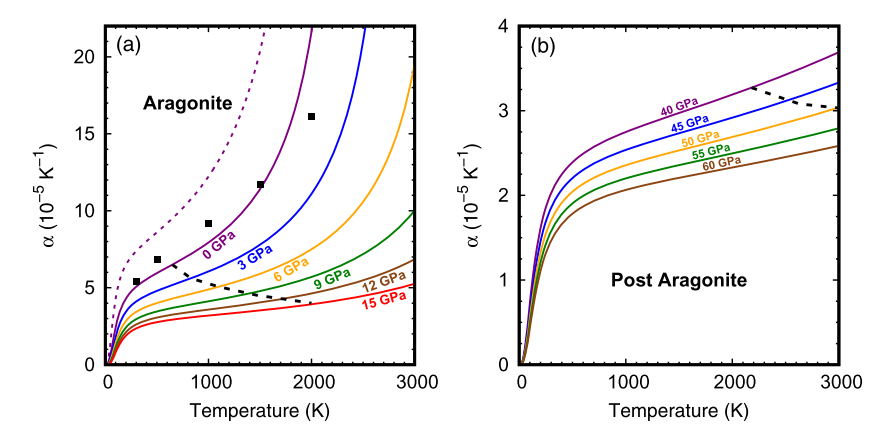


**Fig. 1.** Thermal expansion coefficient at several pressures as a function of temperature for CaCO<sub>3</sub> in (a) aragonite and (b) post-aragonite phases. The dashed lilac line on frame (a) represents the results obtained with the GGA-PBE functional at 0 GPa. The QHA boundary is defined by the position of the inflection points of  $\alpha$ (P,T) (dashed black line), discussed in section 2.2. Experimental results at 0 GPa are presented with black symbols (Litasov et al., 2017). (For interpretation of the colors in the figure(s), the reader is referred to the web version of this article.)

(Litasov et al., 2017; Wentzcovitch et al., 2010; Dorogokupets, 2007; Li et al., 2006; Karki et al., 2000).

#### 2.3. Crystalline phases

In order to explore the stability of carbon-related minerals, at the thermodynamic conditions of the lower mantle, we initially study several crystalline phases of CaCO<sub>3</sub> and MgCO<sub>3</sub> carbonates and CaSiO<sub>3</sub> and MgSiO<sub>3</sub> silicates in a wide pressure range, by computing their respective enthalpies and Gibbs free energies.

For any mineral at a certain temperature and pressure, the respective stable phase is determined as the one with the lowest Gibbs free energy value, using the theoretical model described in the previous section. Additionally, a mineral follows a phase transition at a certain pressure when the free energy of the stable phase becomes greater than the one of a different phase. Our results on stability and phase transition pressures of several carbonate and silicate minerals are in good agreement with results from other theoretical and experimental investigations (Shim et al., 2002; Oganov et al., 2008; Pickard and Needs, 2015; Lobanov et al., 2017; Tsuchiya et al., 2004; Murakami et al., 2004; Fiquet et al., 2002; Isshiki et al., 2004).

We consider several crystalline phases for CaCO<sub>3</sub>, MgCO<sub>3</sub>, MgSiO<sub>3</sub>, CaSiO<sub>3</sub>, MgO, CaO, SiO<sub>2</sub>, and CO<sub>2</sub>. First of all, MgO is considered only in the rock salt (Fm $\overline{3}$ m) phase, since it has been shown that it remains in that phase up to 227 GPa (Duffy et al., 1995). CO<sub>2</sub> is considered only in the  $\beta$ -cristobalite ( $\overline{14}$ 2d) phase (Datchi et al., 2012). We perform static calculations for several other CO<sub>2</sub> phases and we obtain that the above-mentioned phase is the most stable for pressures above 10 GPa, which is fully consistent with results of another investigation that found this phase for pressures from 19 to 150 GPa (Oganov et al., 2008). Additionally, ignoring those other low-pressure stable phases does not compromise our conclusions on the properties of Earth's lower mantle.

For CaSiO<sub>3</sub>, we consider only the perovskite tetragonal (I/4mnm) phase for all the pressures and temperatures studied here (Shim et al., 2002), since it is the most important phase in the thermodynamic conditions of interest. Moreover, within such conditions, our methodology provides results that comply with the validity criteria described in section 2.2, i.e. the thermal expansion coefficient of this phase does not diverge up to 3000 K.

Fig. 2 shows the stable crystalline phases for all other minerals considered in this investigation, as function of pressure at temperatures of 300 K and 2000 K, in which there are available experimental data for comparison. For CaCO<sub>3</sub> at 300 K between

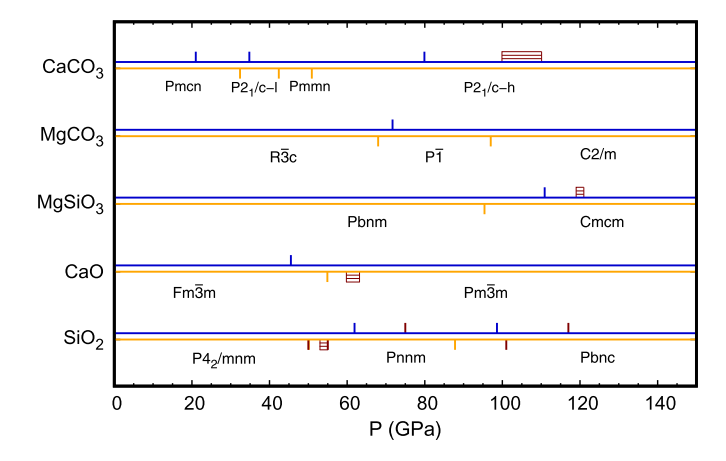


**Fig. 2.** Stable crystalline phases, as function of pressure, of CaCO<sub>3</sub>, MgCO<sub>3</sub>, MgSiO<sub>3</sub>, CaO, and SiO<sub>2</sub> materials considered in this investigation, computed with theoretical approximations presented in section 2.1. The figure presents results for two temperatures: 300 K (orange line) and 2000 K (blue line), with the respective transitions represented by vertical lines. Experimental values for phase transitions, with respective experimental error bars, are presented with brown symbols for: CaCO<sub>3</sub> (Lobanov et al., 2017), MgSiO<sub>3</sub> (Murakami et al., 2004), CaO (Yamanaka et al., 2002), and SiO<sub>2</sub> (Hemley et al., 2000; Andrault et al., 1998; Ono et al., 2002; Murakami et al., 2003).

0 and 150 GPa, the material goes from aragonite (Pmcn) to a monoclinic-low pressure phase (P2 $_1$ /c-l) at 32 GPa, from P2 $_1$ /c-l to post-aragonite (Pmmn) at 42 GPa, and from post-aragonite to a monoclinic-high pressure phase (P2 $_1$ /c-h) at 51 GPa, results that are consistent with another theoretical investigation (Pickard and Needs, 2015). Fig. 2 also shows that, as the temperature increases, there is a major change in the transition pressures. At a high temperature, 2000 K, the post-aragonite to monoclinic-high phase transition occurs at about 80 GPa, in agreement with the theoretical and experimental values of 76 GPa (Pickard and Needs, 2015) and  $105 \pm 5$  GPa (Lobanov et al., 2017), respectively. We observe that when the temperature is increased from 300 K to 2000 K, the value of the phase transition pressure increases by about 30 GPa, showing the relevance of thermal effects when comparing theoretical and experimental results.

For MgCO $_3$  at 300 K, the material goes from magnesite ( $R\overline{3}c$ ) to  $P\overline{1}$  phase at 68 GPa, and from  $P\overline{1}$  phase to magnesite-II (C2/m) at 97 GPa. All these results are in good agreement with other theoretical investigations using static calculations (Pickard and Needs, 2015). We also find that at temperatures over 1850 K, this mineral follows a direct phase transition from magnesite to magnesite-II, i.e. above that temperature the  $P\overline{1}$  phase is not stable at any pres-

sure. Therefore, our results indicate that this phase should be of low geophysical interest for studies of the lower mantle properties

For MgSiO $_3$  at 300 K, the mineral goes from perovskite (Pbnm) to post-perovskite (Cmcm) at 95 GPa, which is consistent with another theoretical investigation (Tsuchiya et al., 2004). At 2000 K, this transition occurs at 111 GPa, in good agreement with the experimental value of 120  $\pm$  3 GPa (Murakami et al., 2004).

For CaO at 300 K, the material goes from rock salt  $(Fm\overline{3}m)$  to CsCl-type phase  $(Pm\overline{3}m)$ . The transition between these two phases is found at 55 GPa, in good agreement with experimental data that identified this transition between 59.8 and 63.2 GPa (Yamanaka et al., 2002).

For  $SiO_2$  at 300 K (2000 K), the material goes from stishovite (P4<sub>2</sub>/mnm) to CaCl<sub>2</sub>-type phase (Pnnm) at 51 GPa (62 GPa), and from CaCl<sub>2</sub>-type phase to columbite-type phase (Pbnc) at 88 GPa (99 GPa). These transition values are in good agreement with experimental data at 300 K (Hemley et al., 2000; Andrault et al., 1998) and 2000 K (Ono et al., 2002; Murakami et al., 2003), as shown in Fig. 2.

#### 3. Results

## 3.1. Decomposition of carbonates at high pressures and temperatures

Most of the Earth's oxidized carbon is expected to be harbored by Mg and/or Ca carbonate forms under mantle pressures and temperatures. In order to identify the potential carbon hosts in this region, we initially explore the energetics associated with the following decomposition reactions:

$$CaCO_3 \Rightarrow CaO + CO_2$$
 (R1)

$$MgCO_3 \Rightarrow MgO + CO_2$$
 (R2)

Fig. 3 shows the relative Gibbs free energy per unit formula (u.f.) as a function of pressure and temperature. It shows that the direct decompositions of  $CaCO_3$  and  $MgCO_3$  into their respective alkaline earth oxides plus  $CO_2$  are unfavorable all over the lower mantle.  $CaCO_3$  and  $MgCO_3$  show similar trends with pressure, i.e., increasing the pressure reduces the Gibbs free energy difference for decomposition, which is positive for all the pressures of interest of the lower mantle. However, the energy cost for the decomposition of  $CaCO_3$  is much greater than the one for  $MgCO_3$ .

It should be stressed that our static results, dashed black line in Fig. 3, are in very good agreement with recent static results (Oganov et al., 2008; Pickard and Needs, 2015), as well as with experimental data (Fiquet et al., 2002). Those researchers have suggested that free  $\rm CO_2$  does not occur as an independent phase within the Earth's mantle. According to the results presented in Figs. 3(a) and (b), temperature effects do not alter the relative stability of carbonates, when compared to their most elementary constituents. Therefore, a temperature increase further reduces the possibility of free  $\rm CO_2$  to exist in that region.

#### 3.2. Stability of carbonates under excess of SiO<sub>2</sub>

We now evaluate the stability of carbonates in a condition of excess of  $SiO_2$ , as represented by reactions (R3) and (R4). This condition is particularly important when one takes into account that there is material mixing in the upper and lower mantle, resulting from the basaltic part of subducting slabs, which is rich in  $SiO_2$  (Oganov et al., 2008).

$$\mathsf{MgCO}_3 + \mathsf{SiO}_2 \Rightarrow \mathsf{MgSiO}_3 + \mathsf{CO}_2 \tag{R3}$$

$$CaCO_3 + SiO_2 \Rightarrow CaSiO_3 + CO_2 \tag{R4}$$

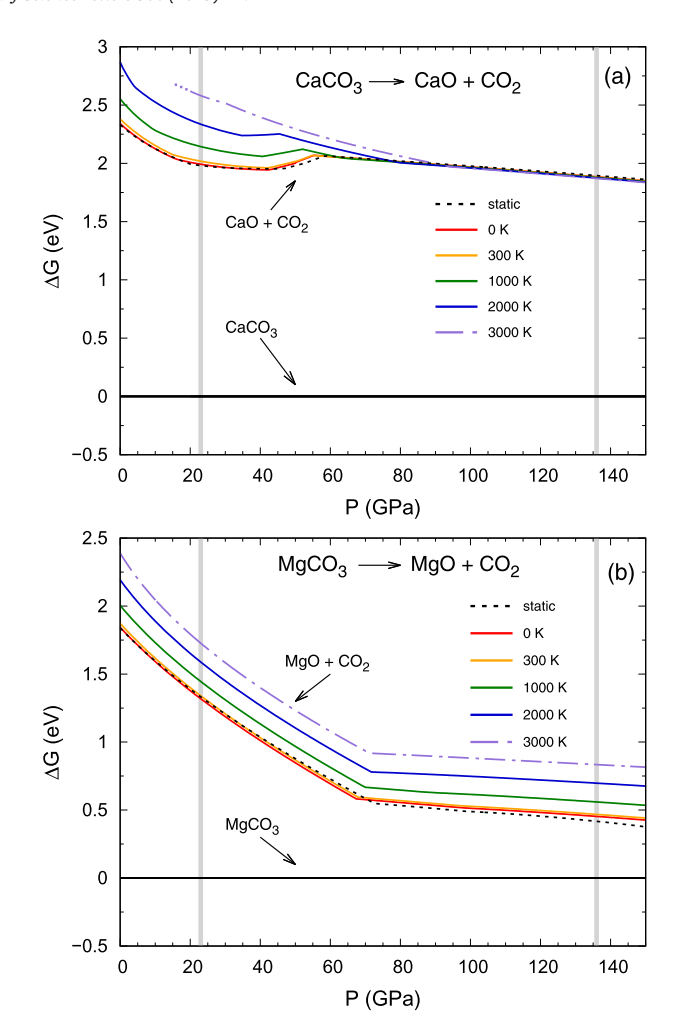


**Fig. 3.** The relative Gibbs free energies per u.f. as function of pressure, at several temperatures, for (a)  $CaCO_3 \rightarrow CaO + CO_2$  and (b)  $CaCO_3 \rightarrow CoO_3 \rightarrow CoO_3$  reactions. The dashed black line represent the respective relative enthalpies. The vertical gray lines indicate the pressures at the top (23 GPa) and bottom (136 GPa) of the lower mantle. The kinks in the curves arise from phase transitions that occur in the minerals described in section 2.3 and shown in Fig. 2, which are used to explore the dissociation reactions.

Fig. 4 shows the relative Gibbs free energies for Mg and Ca carbonates to transform into their respective silicates. The results indicate that reactions (R3) and (R4) are mostly unfavorable, carbonates do not react to form silicates within those thermodynamic conditions. Therefore, there should be no  $\rm CO_2$  formation in the lower mantle as a result of those reactions. Static results in Fig. 4(a) indicate that reaction (R3) is unfavorable up to 127 GPa, i.e. MgCO<sub>3</sub> + SiO<sub>2</sub> is more stable than MgSiO<sub>3</sub> + CO<sub>2</sub>. This pressure is lower than the one in the lower mantle-core boundary of 136 GPa, such that static results suggested that reaction (R3) would be favorable at the bottom of the lower mantle, which could lead to the generation of free CO<sub>2</sub>. The figure shows that reaction (R3) becomes less favorable with increasing temperature, such that this reaction seems unfavorable at typical temperatures of the lower mantle bottom, indicating that free CO<sub>2</sub> is unlikely in this region.

Our static results for reaction (R3), dashed black line in Fig. 4(a), are in good agreement with static results presented in recent theoretical investigations. However, the transition pressure found here (127 GPa) is smaller than the one found by those authors at 135 GPa (Oganov et al., 2008) and 137 GPa (Pickard and Needs, 2015). Such differences could be explained by the functionals used to describe electron–electron interactions, since our investigation uses the LDA, while those investigations use the GGA-PBE. The

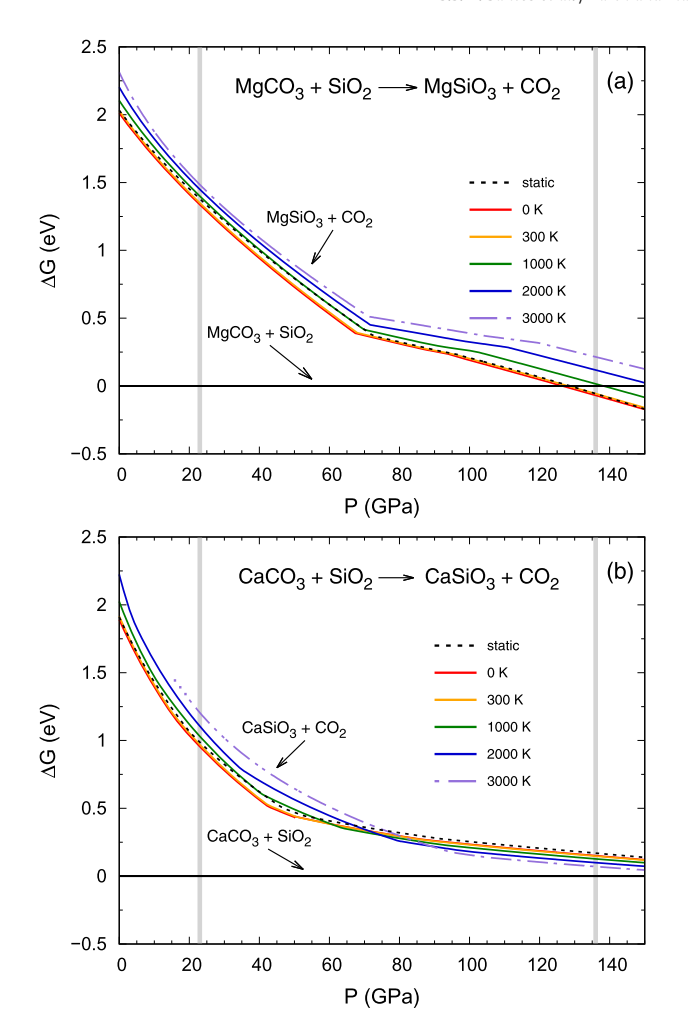


**Fig. 4.** The relative Gibbs free energy per u.f. as function of pressure, at several temperatures, for (a) MgCO $_3$  + SiO $_2$   $\rightarrow$  MgSiO $_3$  + CO $_2$  and (b) CaCO $_3$  + SiO $_2$   $\rightarrow$  CaSiO $_3$  + CO $_2$  reactions. The dashed black line represent the relative enthalpies for the reactions. The vertical gray lines indicate the pressures at the top and bottom of the lower mantle.

choice of LDA over GGA-PBE in this investigation is discussed in detail in section 2.1.

According to Fig. 4(b), the reaction (R4) is energetically unfavorable, i.e.,  $CaCO_3 + SiO_2$  is more stable than  $CaSiO_3 + CO_2$  up to 150 GPa at any temperature. Therefore, in a situation where all these compounds are available,  $CaCO_3$  formation is more likely than  $CaSiO_3$ . Since this pressure is greater than the ones at the bottom of the lower mantle, this reaction would not occur in that region. Our static results are in good agreement with those of another investigation (Pickard and Needs, 2015).

It should be pointed out that our investigation carries some uncertainties on the transition pressures of  $SiO_2$ , as shown in Fig. 2, which could play some role on the final conclusions about the reactions (R3) and (R4), specially on the properties near the coremantle boundary.

## 3.3. Stability of carbonates under excess of MgO or MgSiO<sub>3</sub>

It is reasonably well established that MgO and MgSiO<sub>3</sub> are the two major minerals in the lower mantle. Therefore, it is important to study the stability of MgCO<sub>3</sub> or CaCO<sub>3</sub> in a rich environment with those two minerals. To explore these conditions, we evaluate the energetics associated with reactions (R5) and (R6).

$$MgCO_3 + CaO \Rightarrow CaCO_3 + MgO$$
 (R5)

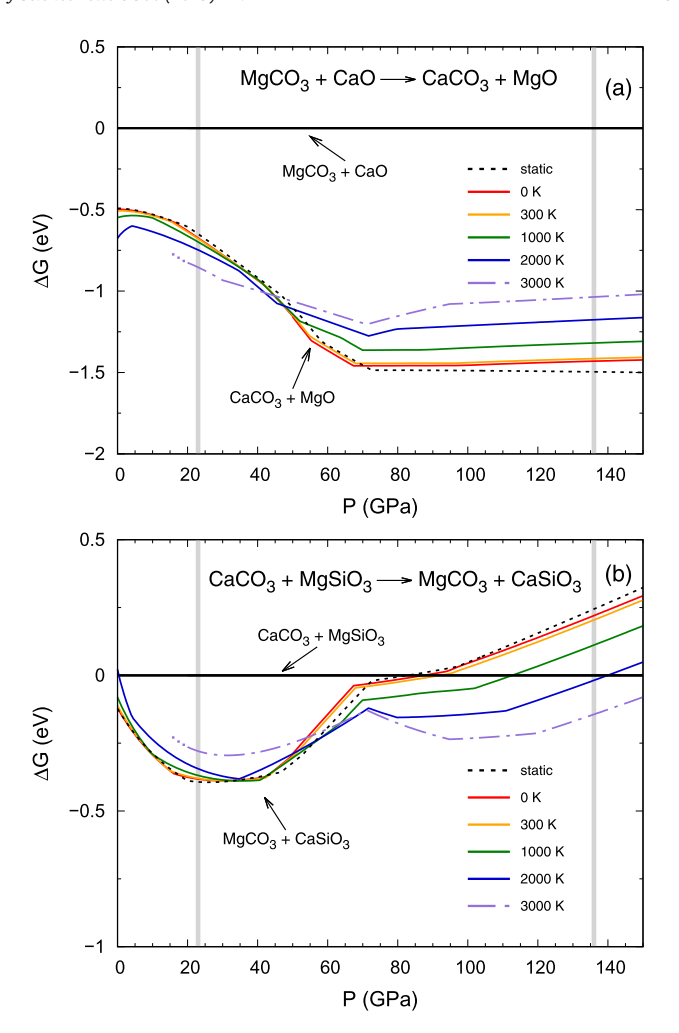


**Fig. 5.** The relative Gibbs free energy per u.f. as function of pressure, at several temperatures, for (a)  $MgCO_3 + CaO \rightarrow CaCO_3 + MgO$  and (b)  $CaCO_3 + MgSiO_3 \rightarrow MgCO_3 + CaSiO_3$  reactions. The dashed black line represent the relative enthalpies in (a) and (b). The vertical gray lines indicate the pressures at the top and bottom of the lower mantle.

$$CaCO_3 + MgSiO_3 \Rightarrow MgCO_3 + CaSiO_3$$
 (R6)

Fig. 5(a) shows that the reaction (R5) is energetically favorable, i.e. CaCO<sub>3</sub> + MgO is more stable than MgCO<sub>3</sub> + CaO, at lower mantle conditions. Although by increasing the temperature, the relative Gibbs free energy is reduced, this effect is not large enough to change the stability of MgCO<sub>3</sub>. Therefore, when there is MgO in excess, as expected in a pyrolitic mantle, CaCO<sub>3</sub> is the stable carbonate under those thermodynamic conditions. Additionally, our static results are in good agreement with recent results (Oganov et al., 2008; Pickard and Needs, 2015).

We now explore the conditions of MgSiO<sub>3</sub> excess, which is the main mineral in the lower mantle. Fig. 5(b) shows that reaction (R6) presents a much richer phenomenology than reaction (R5) across the pressure range of interest. The results of our static calculations show that MgCO<sub>3</sub> + CaSiO<sub>3</sub> is more favorable than CaCO<sub>3</sub> + MgSiO<sub>3</sub> at low pressures, while at pressures greater than 84 GPa, CaCO<sub>3</sub> + MgSiO<sub>3</sub> becomes favorable. Analogously to the reaction (R3), the transition pressure found here is lower than the one found by other authors at 135 GPa (Oganov et al., 2008) and 100 GPa (Pickard and Needs, 2015). However, as the figure shows, there is a dramatic change in the behavior of the reaction (R6) at high temperatures. An increase in temperature increases the pressure in which such reaction could be favorable.

For typical lower mantle temperatures, of at least 2000 K, the reaction (R6) is not favorable anymore. Therefore, the results in

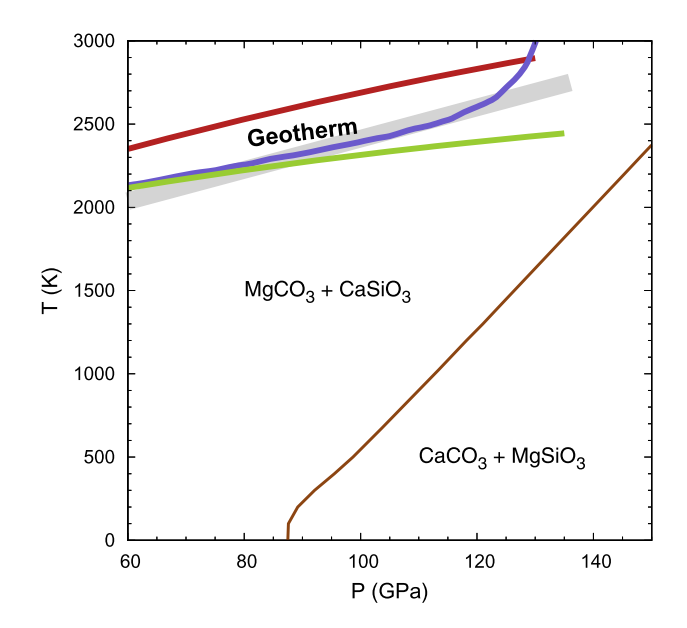


**Fig. 6.** Phase diagram for the stability (brown line) of  $MgCO_3 + CaSiO_3$  versus  $CaCO_3 + MgSiO_3$ . The figure also shows several geotherms: thick gray (Isshiki et al., 2004), green (Brown and Shankland, 1981), blue (Boehler, 2000), and red (Anderson, 1982) lines.

Fig. 5(b) indicate that, at lower mantle conditions under an excess of MgSiO<sub>3</sub>, carbonates appear to be favorable in the form of MgCO<sub>3</sub>. This conclusion is consistent with an experimental investigation (Isshiki et al., 2004), which suggested MgCO<sub>3</sub> as the main oxidized carbon host in the Earth's mantle.

Fig. 6 shows the phase diagram for reaction (R6), along with some Earth's geotherms (Isshiki et al., 2004; Brown and Shankland, 1981; Boehler, 2000; Anderson, 1982). According to the figure, all geotherms lie in the region of stability of  $MgCO_3$ , indicating this mineral as the most likely carbon host in the lower mantle, as expected in a pyrolitic mantle. However, it should be pointed out that there is still controversy on the values of the temperatures at the lower mantle bottom and, therefore, the stability of  $CaCO_3$  over  $MgCO_3$  would require a much colder mantle.

## 4. Summary

This investigation explores the stability of MgCO<sub>3</sub> and CaCO<sub>3</sub> in the thermodynamic conditions of the Earth's lower mantle. The results indicate that a direct decomposition of those carbonates is unfavorable at high temperatures and pressures. Assuming an iron-free pyrolitic lower-mantle composition, the investigation also explores the stability of those carbonates in conditions of excess of SiO<sub>2</sub>, MgO, and MgSiO<sub>3</sub>.

In a MgO-rich environment, the results show that CaCO<sub>3</sub> + MgO is more stable than  $MgCO_3 + CaO$ , and the relative energy reduction with increasing temperature is not large enough to change the stability of CaCO<sub>3</sub>. On the other hand, in a MgSiO<sub>3</sub>-rich environment, the static results show that at the upper half of the lower mantle, MgCO<sub>3</sub> + CaSiO<sub>3</sub> is more favorable than CaCO<sub>3</sub> + MgSiO<sub>3</sub>, while at pressures greater than 84 GPa, the latter becomes favorable. However, when the effects of temperature are taken into account, this behavior changes dramatically and the increase in temperature increases the value of the pressure at which this reaction (R6) becomes favorable and, finally, the magnesium carbonate turns out to be more stable than the calcium carbonate. Consequently, the incorporation of the temperature effects leads to the situation where calcium carbonate should not be considered as a host of the subducted carbon, in contrast to the conclusions of static calculations (Pickard and Needs, 2015), which suggested a

competition between those two carbonates as carbon hosts in the lower mantle.

Since magnesium silicate is the main component of a pyrolitic mantle, it can be inferred that carbonates appear to be favorable in the form of MgCO<sub>3</sub>. Therefore, the magnesium carbonate should be the main host of oxidized carbon in most of the lower mantle. Only at the bottom of the mantle or in a region with an excess of MgO that calcium carbonate could become preferable. However, at the bottom of the mantle, this carbonate would be favorable only considering geotherms with a very low increase in temperature close to the core–mantle boundary.

The results also show that both carbonates do not decompose into their respective alkaline earth oxides plus  $\mathrm{CO}_2$  through the entire lower mantle, which indicates a low concentration of free carbon dioxide in those regions. However, the decomposition reaction of  $\mathrm{MgCO}_3$  into  $\mathrm{MgO} + \mathrm{CO}_2$  would only be possible very close to the core–mantle boundary. Furthermore, free  $\mathrm{CO}_2$  could be produced in an environment with an excess of  $\mathrm{SiO}_2$ , as in small silica-rich basaltic parts of the subducted slabs.

All those results add a new evidence for the presence of carbon on the deep mantle in the form of carbonates (Hazen and Schiffries, 2013; Marcondes et al., 2016). However, it is still uncertain how the presence of iron, and its rich phenomenology associated to spin transition at high pressures (Wentzcovitch et al., 2009; Liu et al., 2015), would affect the stability of carbonates in the lower mantle. Moreover, the decomposition of CO<sub>2</sub> into diamond plus oxygen should be explored to enrich the discussion of the presence of carbon in the deep mantle in a reduced state.

## Acknowledgements

This investigation is supported by the Brazilian agencies CNPq (grant numbers 305753/2017-7, 303745/2014-2, 140042/2014-8, and 158030/2012-5) and CAPES (grant number BEX 14456/13-3). We acknowledge resources from the Blue Gene/Q supercomputer supported by the Center for Research Computing (Rice University) and the Superintendência de Tecnologia da Informação (Universidade de São Paulo).

### References

Anderson, O.L., 1982. The Earth's core and the phase diagram of iron. Philos. Trans. R. Soc. Lond. A 306, 21–35.

Andrault, D., Fiquet, G., Guyot, F., Hanfland, M., 1998. Pressure-induced Landau-type transition in stishovite. Science 282, 720–724.

Baroni, S., de Gironcoli, S., Dal Corso, A., Giannozzi, P., 2001. Phonons and related crystal properties from density-functional perturbation theory. Rev. Mod. Phys. 73, 515–562.

Blochl, P.E., 1994. Projector augmented-wave method. Phys. Rev. B 50, 17953–17979. Boehler, R., 2000. High-pressure experiments and the phase diagram of lower mantle and core materials. Rev. Geophys. 38, 221–245.

Brown, J.M., Shankland, T.J., 1981. Thermodynamic parameters in the Earth as determined from seismic profiles. Geophys. J. Int. 66, 579–596.

Burton, M.R., Sawyer, G.M., Granieri, D., 2013. Deep carbon emissions from volcanoes. Rev. Mineral. Geochem. 75, 323–354.

Carrier, P., Wentzcovitch, R., Tsuchiya, J., 2007. First-principles prediction of crystal structures at high temperatures using the quasiharmonic approximation. Phys. Rev. B 76, 064116.

Datchi, F., Mallick, B., Salamat, A., Ninet, S., 2012. Structure of polymeric carbon dioxide CO<sub>2</sub>-V. Phys. Rev. Lett. 108, 125701.

Dorogokupets, P.I., 2007. Equation of state of magnesite for the conditions of the Earth's lower mantle. Geochem. Int. 45, 561–568.

Duffy, T.S., Hemley, R.J., Mao, H.-k., 1995. Equation of state and shear strength at multimegabar pressures: magnesium oxide to 227 GPa. Phys. Rev. Lett. 74, 1371–1374.

Fiquet, G., Guyot, F., Kunz, M., Matas, J., Andrault, D., Hanfland, M., 2002. Structural refinements of magnesite at very high pressure. Am. Mineral. 87, 1261–1265.

Gavryushkin, P.N., Martirosyan, N.S., Inerbaev, T.M., Popov, Z.I., Rashchenko, S.V., Likhacheva, A.Y., Lobanov, S.S., Goncharov, A.F., Prakapenka, V.B., Litasov, K.D., 2017. Aragonite-II and CaCO<sub>3</sub>-VII: new high-pressure, high-temperature polymorphs of CaCO<sub>3</sub>. Cryst. Growth Des. 17, 6291–6296.

- Giannozzi, P., Baroni, S., Bonini, N., Calandra, M., Car, R., Cavazzoni, C., Ceresoli, D., Chiarotti, G.L., Cococcioni, M., Dabo, I., Dal Corso, A., de Gironcoli, S., Fabris, S., Fratesi, G., Gebauer, R., Gerstmann, U., Gougoussis, C., Kokalj, A., Lazzeri, M., Martin-Samos, L., Marzari, N., Mauri, F., Mazzarello, R., Paolini, S., Pasquarello, A., Paulatto, L., Sbraccia, C., Scandolo, S., Sclauzero, G., Seitsonen, A.P., Smogunov, A., Umari, P., Wentzcovitch, R.M., 2009. QUANTUM ESPRESSO: a modular and opensource software project for quantum simulations of materials. J. Phys. Condens. Matter 21, 395502.
- Hazen, R.M., Schiffries, C.M., 2013. Why deep carbon? Rev. Mineral. Geochem. 75, 1. Hemley, R.J., Shu, J., Carpenter, M.A., Hu, J., Mao, H.K., Kingma, K.J., 2000. Strain/order parameter coupling in the ferroelastic transition in dense SiO<sub>2</sub>. Solid State Commun. 114, 527–532.
- Holzwarth, N.A.W., Tackett, A.R., Matthews, G.E., 2001. A projector augmented wave (PAW) code for electronic structure calculations, part I: atompaw for generating atom-centered functions. Comput. Phys. Commun. 135, 329–347.
- Isshiki, M., Irifune, T., Hirose, K., Ono, S., Ohishi, Y., Watanuki, T., Nishibori, E., Takata, M., Sakata, M., 2004. Stability of magnesite and its high-pressure form in the lowermost mantle. Nature 427, 60–63.
- Jones, A.P., Genge, M., Carmody, L., 2013. Carbonate melts and carbonatites. Rev. Mineral. Geochem. 75, 289.
- Karki, B.B., Wentzcovitch, R.M., de Gironcoli, S., Baroni, S., 2000. Ab initio lattice dynamics of MgSiO<sub>3</sub> perovskite at high pressure. Phys. Rev. B 62, 14750–14756.
- Kohn, W., Sham, L.J., 1965. Self-consistent equations including exchange and correlation effects. Phys. Rev. 140, A1133–A1138.
- Li, L., Weidner, D.J., Brodholt, J., Alfè, D., Price, G.D., Caracas, R., Wentzcovitch, R., 2006. Elasticity of CaSiO<sub>3</sub> perovskite at high pressure and high temperature. Phys. Earth Planet. Inter. 155, 249–259.
- Litasov, K.D., Shatskiy, A., Gavryushkin, P.N., Bekhtenova, A.E., Dorogokupets, P.I., Danilov, B.S., Higo, Y., Akilbekov, A.T., Inerbaev, T.M., 2017. P-V-T equation of state of CaCO<sub>3</sub> aragonite to 29 GPa and 1673 K: in situ X-ray diffraction study. Phys. Earth Planet. Inter. 265, 82.
- Liu, J., Lin, J.-F., Prakapenka, V.B., 2015. High-pressure orthorhombic ferromagnesite as a potential deep-mantle carbon carrier. Sci. Rep. 5, 7640.
- Lobanov, S.S., Dong, X., Martirosyan, N.S., Samtsevich, A.I., Stevanovic, V., Gavryushkin, P.N., Litasov, K.D., Greenberg, E., Prakapenka, V.B., Oganov, A.R., Goncharov, A.F., 2017. Raman spectroscopy and X-ray diffraction of  $sp^3$  CaCO<sub>3</sub> at lower mantle pressures. Phys. Rev. B 96, 104101.
- Maeda, F., Ohtani, E., Kamada, S., Sakamaki, T., Hirao, N., Ohishi, Y., 2017. Diamond formation in the deep lower mantle: a high-pressure reaction of MgCO<sub>3</sub> and SiO<sub>2</sub>. Sci. Rep. 7, 40602.
- Marcondes, M.L., Justo, J.F., Assali, L.V.C., 2016. Carbonates at high pressures: possible carriers for deep carbon reservoirs in the Earth's lower mantle. Phys. Rev. B 94, 104112.
- Marcondes, M.L., Wentzcovitch, R.M., Assali, L.V.C., 2018. Importance of van der Waals interaction on structural, vibrational, and thermodynamic properties of NaCl. Solid State Commun. 273, 11–16.
- Marty, B., Alexander, C.M.O., Raymond, S.N., 2013. Primordial origins of Earth's carbon. Rev. Mineral. Geochem. 75, 149.
- Murakami, M., Hirose, K., Kawamura, K., Sata, N., Ohishi, Y., 2004. Post-perovskite phase transition in MgSiO<sub>3</sub>. Science 304, 855.
- Murakami, M., Hirose, K., Ono, S., Ohishi, Y., 2003. Stability of  $CaCl_2$ -type and  $\alpha$ -PbO<sub>2</sub>-type  $SiO_2$  at high pressure and temperature determined by in-situ X-ray measurements. Geophys. Res. Lett. 30, 1207.

- Oganov, A.R., Hemley, R.J., Hazen, R.M., Jones, A.P., 2013. Structure, bonding, and mineralogy of carbon at extreme conditions. Rev. Mineral. Geochem. 75, 47–77.
- Oganov, A.R., Ono, S., Ma, Y., Glass, C.W., Garcia, A., 2008. Novel high-pressure structures of MgCO<sub>3</sub>, CaCO<sub>3</sub> and CO<sub>2</sub> and their role in Earth's lower mantle. Earth Planet. Sci. Lett. 273. 38–47.
- Ono, S., Hirose, K., Murakami, M., Isshiki, M., 2002. Post-stishovite phase boundary in SiO<sub>2</sub> determined by in situ X-ray observations. Earth Planet. Sci. Lett. 197, 187–192.
- Pearson, D.G., Brenker, F.E., Nestola, F., McNeill, J., Nasdala, L., Hutchison, M.T., Matveev, S., Mather, K., Silversmit, G., Schmitz, S., Vekemans, B., Vincze, L., 2014. Hydrous mantle transition zone indicated by ringwoodite included within diamond. Nature (London) 507, 221.
- Perdew, J.P., Burke, K., Ernzerhof, M., 1996. Generalized gradient approximation made simple. Phys. Rev. Lett. 77, 3865–3868.
- Pickard, C.J., Needs, R.J., 2015. Structures and stability of calcium and magnesium carbonates at mantle pressures. Phys. Rev. B 91, 104101.
- Shcheka, S.S., Wiedenbeck, M., Frost, D.J., Keppler, H., 2006. Carbon solubility in mantle minerals. Earth Planet. Sci. Lett. 245, 730–742.
- Shim, S., Jeanloz, R., Duffy, T.S., 2002. Tetragonal structure of CaSiO<sub>3</sub> perovskite above 20 GPa. Geophys. Res. Lett. 29, 2166.
- Shirasaka, M., Takahashi, E., Nishihara, Y., Matsukage, K., Kikegawa, T., 2002. In situ X-ray observation of the reaction dolomite = aragonite + magnesite at 900–1300 K. Am. Mineral. 87, 922.
- Shirey, S.B., Cartigny, P., Frost, D.J., Keshav, S., Nestola, F., Nimis, P., Pearson, D.G., Sobolev, N.V., Walter, M.J., 2013. Diamonds and the geology of mantle carbon. Rev. Mineral. Geochem. 75, 355.
- Smith, D., Lawler, K.V., Martinez-Canales, M., Daykin, A.W., Fussell, Z., Smith, G.A., Childs, C., Smith, J.S., Pickard, C.J., Salamat, A., 2018. Postaragonite phases of CaCO<sub>3</sub> at lower mantle pressures. Phys. Rev. Mater. 2, 013605.
- Tsuchiya, T., Tsuchiya, J., Umemoto, K., Wentzcovitch, R.M., 2004. Phase transition in MgSiO<sub>3</sub> perovskite in the Earth's lower mantle. Earth Planet. Sci. Lett. 224, 241, 248
- Walter, M.J., Kohn, S.C., Araujo, D., Bulanova, G.P., Smith, C.B., Gaillou, E., Wang, J., Steele, A., Shirey, S.B., 2011. Deep mantle cycling of oceanic crust: evidence from diamonds and their mineral inclusions. Science 334, 54–57.
- Wang, Y., Wang, J.J., Wang, W.Y., Mei, Z.G., Shang, S.L., Chen, L.Q., Liu, Z.K., 2010.
  A mixed-space approach to first-principles calculations of phonon frequencies for polar materials. J. Phys. Condens. Matter 22, 202201.
- Wentzcovitch, R.M., Justo, J.F., Wu, Z., da Silva, C.R.S., Yuen, D.A., Kohlstedt, D., 2009. Anomalous compressibility of ferropericlase throughout the iron spin cross-over. Proc. Natl. Acad. Sci. USA 106, 8447–8452.
- Wentzcovitch, R.M., Karki, B.B., Cococcioni, M., de Gironcoli, S., 2004. Thermoelastic properties of MgSiO<sub>3</sub>-perovskite: insights on the nature of the Earth's lower mantle. Phys. Rev. Lett. 92, 18501.
- Wentzcovitch, R.M., Martins, J.L., Price, G.D., 1993. Ab initio molecular dynamics with variable cell shape: application to MgSiO<sub>3</sub>. Phys. Rev. Lett. 70, 3947–3951.
- Wentzcovitch, R.M., Yu, Y.G., Wu, Z., 2010. Thermodynamic properties and phase relations in mantle minerals investigated by first principles quasiharmonic theory. Rev. Mineral. Geochem. 71, 59.
- Yamanaka, T., Kittaka, K., Nagai, T., 2002. B1–B2 transition in CaO and possibility of CaSiO<sub>3</sub>-perovskite decomposition under high pressure. J. Mineral. Petrol. Sci. 97 (4), 144–152.